Supporting Information

Nanobowl-Supported Liposomes Improve Drug Loading and Delivery

Zhong-Jian Chen,[†,#] Si-Cong Yang,[†,#] Xue-Liang Liu,[†] Yuhao Gao,[†] Xiao Dong,[†] Xing Lai,[†] Mao-Hua Zhu,[†] Hai-Yi Feng,[†] Xin-Di Zhu,[†] Qin Lu,[†] Mei Zhao,[‡] Hong-Zhuan Chen,[§] Jonathan F. Lovell,[,∥] and Chao Fang[*,†]*

[†] Hongqiao International Institute of Medicine, Tongren Hospital and State Key Laboratory of Oncogenes and Related Genes, Department of Pharmacology and Chemical Biology, Shanghai Jiao Tong University School of Medicine (SJTU-SM), Shanghai 200025, China

[‡] Department of Pharmacy, Shanghai University of Medicine and Health Sciences, 279 Zhouzhu Road, Shanghai 201318, China

[§] Institute of Interdisciplinary Integrative Biomedical Research, Shuguang Hospital, Shanghai University of Traditional Chinese Medicine, Shanghai 201203, China

[∥] Department of Biomedical Engineering, University at Buffalo, State University of New York, Buffalo, NY 14260, USA

[#] Z.-J. Chen, and S.-C. Yang contributed equally to this work.

*Corresponding Author:

Chao Fang (fangchao32@sjtu.edu.cn) and Jonathan F. Lovell (jflovell@buffalo.edu)

Experimental Details

Materials, Cell Culture, and Animals.

Styrene, 3-trimethoxysilylpropyl methacrylate (MPS), sodium 4-vinylbenzenesulfonate (VBS), tetraethyl orthosilicate (TEOS, 98%), N-(3-trimethoxysilylpropyl) diethylenetriamine, (3-aminopropyl) triethoxysilane, and sulforhodamine B (SRB) were purchased from Sigma-Aldrich (St. Louis, MO). Ammonium hydroxide solution (25% NH_3), 2,2'-azobis 2-methylpropionitrile (AIBN), potassium peroxodisulfate (KPS), sodium dodecyl sulfate (SDS), tetrahydrofuran (THF) and ammonium sulfate were purchased from J&K Scientific Company (Shanghai, China). Doxorubicin hydrochloride, irinotecan, vincristine sulfate and trifluoroacetic acid (HPLC grade) were purchased from Aladdin Chemicals (Shanghai, China). L-α-phosphatidylcholine, hydrogenated (Soy) (HSPC), cholesterol (ovine) and 1, 2-distearoyl-sn-glycero-3- phosphoethanolamine-N-[methoxy- (polyethylene glycol)-2000] (ammonium salt) (mPEG2000- DSPE), sphingomyelin (Egg, chicken), 1,2-distearoyl-sn-glycero-3-phosphocholine (DSPC) were purchased from Avanti Polar Lipids (Alabama, USA). PCNA cell proliferation kit and dialysis bag (MWCO 3.5 kDa) were purchased from Sangon Biotech (Shanghai, China). Streptomycin, penicillin, sodium pyruvate, trypsin, Hoechst 33342, Alexa Fluor 647 phalloidin, 1,1'-dioctadecyl-3,3,3',3'-tetramethylindotricarbocyanine iodide (DiR), zeba spin desalting columns (MWCO 7 kDa), Dulbecco's modified Eagle medium (DMEM) and Dulbecco's phosphate-buffered saline (DPBS) were obtained from ThermoFisher Scientific (Shanghai, China). Fetal bovine serum (FBS) was purchased from Gemini Bio Products. Methanol (HPLC grade), acetonitrile (HPLC grade), isopropyl alcohol (HPLC grade) were purchased from TEDIA, USA. Ultrapure water was obtained from a Millipore Milli-Q system (Bedford, MA). All other chemicals were of analytical grade and used without further purification.

Mouse 4T1 breast cancer cell line was purchased from ATCC (Manassas, VA). 4T1-luc cells (4T1 transfected with luciferase) were established by Shanghai Model Organisms Center (China). The cells were cultured in DMEM supplemented with 10% FBS, 100 $U \cdot mL^{-1}$ penicillin, and 100 $\mu g \cdot mL^{-1}$ streptomycin and in the incubator containing 5% CO_2 under 37 °C.

BALB/c mice (female, age of 7-8 weeks) were obtained from Shanghai Laboratory Animal Center (China). All animal-involved experiments were approved by the IACUC of Shanghai Jiao Tong University School of Medicine.

Preparation and Characterization of DOX@NbLipo.

The Janus silica nanobowls were synthesized as described in the literature,[1] where 50 nm polystyrene nanoparticles (PS-NP) were produced through emulsion polymerization[2-4] as the original seeds. Nanobowls were obtained through dissolution of the polymeric template using tetrahydrofuran (THF).

For the surface amination of the nanobowls, 5 mg nanobowls in 25 mL ethanol were mixed with 0.5 mL of NH_3 and 0.1 mL of N-(3-trimethoxysilylporpyl) diethylenetriamine. The mixture was magnetically stirred at 500 rpm overnight to result in the aminated nanobowls (NH_2-Nanobowl).

To prepare nanobowl-supported liposomes, 5 mg NH_2-nanobowls in 5 mL 300 mM ammonium sulfate solution were added to the lipid (10 mg) thin film coated on a round-bottom flask for 1 h hydration (60 ℃, 200 rpm). Then, probe sonication was performed for 30 min, with a 15/15 s on/off working cycle and output 40 w power (JY92-II, Scientz Biotechnology, Ningbo, China) to generate nanobowl-

supported liposomes (NbLipo). Then, external ammonium sulfate was replaced with a pH 6.5 sucrose solution (300 mM) containing 10 mM histidine through dialysis at 4 ℃ for 24 h. The empty NbLipo were collected through centrifugation (24000 g, 20 min) and the associated lipid was quantified using the method described in the literature.[5]

For DOX loading, doxorubicin hydrochloride dissolved in sucrose solution (300 mM sucrose, 10 mM L-histidine, pH 6.5) was mixed with the empty NbLipo at a various drug-to-lipid ratios (0.05, 0.1, 0.2, and 0.5). Then, the mixture was incubated at 60 ℃ in a water bath for 1 h, and cooled down in ice water for 5 min. The DOX-loaded NbLipo (DOX@NbLipo) were collected through centrifugation at 24,000 g for 20 min, washed for three times using sucrose solution, and stored at 4 ℃ with protection from light. The encapsulation efficiency of DOX was estimated through determining the liposome-associated DOX content using fluorescence spectroscopy.

The irinotecan or vincristine loaded NbLipo was also prepared respectively using the same methods. For comparison, drugs (DOX, irinotecan, and vincristine) loaded in the conventional liposomes (Lipo) with no embedded nanobowl were prepared using the classical methods of lipid film hydration, extrusion through mini-extruder, and transmembrane pH gradient-driven loading. For all liposome preparations, the lipid composition was as following: 95.8 mg HSPC, 31.9 mg cholesterol, and 31.9 mg mPEG2000-DSPE (56.3:38.4:5.3, molar ratio same to Doxil) for liposomal DOX,[6] 68.1 mg DSPC, 22.2 mg cholesterol, and 1.2 mg mPEG2000-DSPE (3:2:0.015, molar ratio same to Onivyde) for liposomal irinotecan,[7] and 60 mg Egg SM and 29.5 mg cholesterol (60:40, molar ratio same to Marqibo) for liposomal vincristine.[8]

Hydrodynamic size and zeta potential of the nanoparticles and liposomes were measured through dynamic light scattering (DLS) by ZetaSizer Nano ZS instrument (Malvern, Worcestershire, UK). The morphology and structure of the nanoparticles and liposomes were also observed using transmission electron microscopy (TEM, Tecnai G2 SpiritBiotwin, USA) or cryo-EM (Talos F200C, USA).

To identify the structure and integrity of DOX@NbLipo, the nanobowl (aminated) was labeled with Alexa Fluor 647 NHS ester, and the liposomal bilayer was labeled with DiR to generate dual-fluorophore-labeled DOX@NbLipo (Alexa Fluor 647, DiR). The specific Vis-NIR absorption and FRET signal of DOX@NbLipo (Alexa Fluor 647, DiR) was examined and observed using both SpectraMAX M2 microplate reader (Molecular Devices) and IVIS spectrum CT instrument (PerkinElmer).

Detection of Young's Modulus.

For sample preparation, megohmit was previously coated with poly-lysine (0.05 mg/mL). Then, empty Lipo or NbLipo was dropped onto the megohmit for their adhesion to the megohmit surface. The megohmit was then rinsed with Milli-Q water twice to remove the nonadherent liposomes. AFM images were obtained using Dimension FastScan Bio Atomic Force Microscopy (AFM, Bruker). ScanAsyst mode using MLCT probe with a spring constant of 0.1 N/m was used. The scanning rate was 4 kHz. The Young's modulus of the liposomes was estimated using the NanoScope analysis software (Bruker, USA).[9-10]

Differential Scanning Calorimetry (DSC) Assay

DSC assay was performed using a Nano DSC instrument (TA Instruments, New Castle, DE, USA) to

identify the DOX status in the liposomes (DOX@Lipo and DOX@NbLipo). Scanning was carried out on aliquots of 0.9 ml of the liposome samples with 10% sucrose in 10 mM histidine buffer (pH 6.5) as the reference. Heating from 10 °C to 90 °C at the rate of 1.0 °C/min. The distinct endotherms were compared with those of Doxil reported in the literature.[11]

Drug Leakage Induced by Serum.

To examine the serum-induced membrane instability and cargo leakage, sulforhodamine B (SRB), a hydrophilic fluorescent cargo, was loaded into the liposomal water cavity at 50 mM (a self-quenching concentration).[12] The resultant SRB-encapsulated Lipo or NbLipo were dispersed in pure FBS at 37 ℃ and shaken at 200 rpm. SRB fluorescence (Ex 490 nm, Em 590 nm) was monitored at pre-determined time point using a SpectraMAX M2 microplate reader (Molecular Devices). The increased SRB fluorescence indicated the cargo leakage from the water cavity of the liposomes.

To quantify DOX leakage, DOX@NbLipo after FBS incubation for a specified time were purified using Zebaspin desalting columns (Thermo Scientific) to remove the DOX outside of the liposomes. Liposomes with the retained DOX was mixed with 9-fold volume of 0.75 M HCL (containing 90% isopropyl alcohol), and the DOX was quantified through fluorescent assay (Ex 490 nm, Em 590 nm). DOX leakage caused by FBS was then estimated by subtracting the drug retained in the liposomes.

For the assay of irinotecan or vincristine leakage, liposomes with retained drug was mixed with 9-fold volume 0.75 M HCL (containing 90% isopropyl alcohol). Then, the supernatant containing irinotecan or vincristine was volatilized in a SpeedVac Concentrator (Thermo Scientific) and the residues were

resolved in 200 μL mobile phase, which was composed of methanol, acetonitrile, water and trifluoroacetic acid at 24:24:52:0.1 (v/v, pH = 3.0) for HPLC assay at flow rate of 1 mL/min. A diamonsil C18 column (4.6×150 mm, 5 μm, Dikma, China) was used for separation, and detection was performed at 254 nm.

Drug Leakage Induced by Shear Stress.

Liposomes (Lipo or NbLipo) loaded with DOX or self-quenched SRB (50 mM) were dispersed in FBS and placed in the sample cup of Brookfield DV3TLVCP viscometer (Ametek, USA). A DG-3 float rotor was equipped to confer a shear rate of 1500 s^{-1}, which corresponded to a shear stress of ~ 55 dyne/cm^2 in the context of normal arterioles.[13] The sample temperature was maintained at 37 ℃ using a Brookfield circulating water bath. At the time point of 1, 2, and 4 h, 1 mL sample was taken out for the leakage assay as described above.

Forster Resonance Energy Transfer (FRET) observation.

To examine liposome fusion under FBS, the liposomes (Lipo and NbLipo) were labeled with DiO (FRET donor) and DiI (FRET acceptor), respectively. Then, liposomes with equal concentration (0.16 μg/mL) of DiO or DiI were mixed and dispersed in FBS, and shaken at 200 rpm at 37 ℃. At pre-determined time point, FRET signal and intensity (Ex 410 nm, Em 560 nm) of the mixture was detected using a SpectraMAX M2 microplate reader (Molecular Devices). FRET assay was also performed in the context of shear stress as mentioned above.

In Vitro Cellular Uptake.

4T1 cells (5×10^3) were seeded in glass ground cell culture dish. After 24 h incubation, culture medium containing DOX@NbLipo or DOX@Lipo at DOX concentration of 10 μg/mL was added for another 2 or 4 h incubation. Then, cell nuclei were stained with Hoechst 33342 (Ex 405 nm, Em 450~460 nm) and cell F-actin was labeled with Alexa Fluor 647 phalloidin (Ex 633 nm, Em 665 nm). The fluorescent intracellular DOX (Ex 488 nm, Em 590 nm) were observed under CLSM (Leica TCS SP8 STED 3X, Germany). The cell-associated DOX were also quantified using flow cytometry (Beckman Coulter CytoFLEX S) (Ex 488 nm, Em 585 nm).

Cell Viability.

4T1 cells were seeded in 96-well plates at a density of 5000 cells per well. After 12 h culture, the cell medium was replaced with fresh medium containing DOX, DOX@Lipo, or DOX@NbLipo at DOX dose of 0.01, 0.03, 0.1, 0.3, 1, 3, 10 μg/mL, respectively. After 48 h incubation, cell viabilities were quantitatively detected using Cell Counting Kit-8 (Dojindo, Laboratories, Kumamoto, Japan). The empty NbLipo were set as control.

Cytotoxicity was also qualitatively evaluated using calcein-AM and 7-aminoactinomycin D (7-AAD) dual-staining test.[14] Calcein-AM can be enzymatically converted into green fluorescent calcein in live cells, while the nuclei of dead cells are stained with 7-AAD (red fluorescence). After 48 h incubation with various DOX-contained formulations, cell medium was replaced with PBS containing 0.5 μg mL^{-1} calcein-AM (Ex 488 nm, Em 515 nm) and 5 μg mL^{-1} 7-AAD (Ex 561 nm, Em 615 nm). Then, the cells were photographed under the microscope (Leica TCS SP8).

Blood Clearance Kinetics.

Female BALB/c mice (n = 5) were injected with DOX@NbLipo at DOX dose of 4 mg/kg. At 0.5, 1, 2, 4, 8, 12, 24, and 48 h post injection, 50 μL blood was sampled from orbital vein for DOX quantification as the method described.[15] Briefly, blood was centrifuged at 1500 g for 15 min. 20 μL serum was diluted in extraction buffer (0.075 M HCl containing 90% isopropanol), and DOX was assayed using fluorescent determination (Ex 490 nm, Em 590 nm). The DOX concentration versus time plot was then plotted and the blood half-life was calculated using the WinNonlin software (Version 6.1 Pharsight, Mountain View, CA) according to noncompartmental model.

Orthotopic Tumor Targeting and Biodistribution.

Orthotopic tumor targeting was visualized using an IVIS Spectrum CT multimodal imaging system (PerkinElmer). The mice were i.v. injected with DiD-labeled NbLipo at DiD dose of 0.2 mg/kg. After 24 h, the mice were imaged to detect the liposomal fluorescence signal (Ex 640 nm, Em 660 nm) in the bioluminescent tumor.

Time-dependent tumor targeting and biodistribution were also performed at 24, 48, 72, and 96 h after DiD-labeled liposome injection. Tumors and major organs (heart, liver, spleen, lung, and kidney) were harvested for *ex vivo* imaging. Time-dependent (0~144 h) DOX contents in tumors after DOX@NbLipo injection were also assayed. For DOX quantification, the tumors were homogenized and extracted overnight in hydrofluoric acid, and DOX content was determined by fluorescence detection (Ex 480 nm, Em 590 nm).

Antitumor Therapy in Orthotopic 4T1 Breast Tumor Model.

The orthotopic 4T1 tumor model was established through inoculating 8×10^5 cells (in 50 μL DMEM) into the right fourth mammary fat pad of female BALB/c mice. When tumor grew to ~80 mm^3, mice were randomly divided into four groups and treated with saline, NbLipo (empty), DOX@Lipo and DOX@NbLipo (DOX dose 4 mg/kg) on days 0, 3 and 6, respectively. On day 8, mice from each group (n=3) were sacrificed and tumors and major organs (heart, liver, lung, spleen and kidney) were excised for pathological H&E assay for the antitumor effect and toxicity. Tumor cell proliferation in tumor tissues were examined through PCNA immunohistological staining. All images were taken by Nikon Eclipse E200 photomicroscope and analyzed blindly using Image-Pro Plus 6.0 software (Media Cybernetics, Bethesda, MD). Tumor volume was monitored and calculated as follows: $V = 0.5 \times (length) \times (width)^2$. Survival observation (n=8 per group) was continued until tumor volume reached the ethical limit (2000 mm^3).[16] The increase in life span (*ILS*) was calculated according to the following formula: % *ILS* = (T/C -1) × 100%.[17] T and C are the median survival time of the treated mice and the mice from saline group, respectively. When there was a mouse tumor grew to 2000 mm^3, four mice from each group were sacrificed, and the mouse lungs were harvested for *ex vivo* bioluminescent imaging to examine the metastasis as previously described.[18] Mouse body weight were recorded to evaluate the toxicity.

Blood Analysis.

Healthy female BALB/c mice were intravenously injected with free DOX, DOX@Lipo and DOX@NbLipo (4 mg/kg DOX), respectively, for 3 times on days 0, 3, and 6. On day 9, retro orbital blood collection from 3 mice per group were performed for serum biochemistry assay and complete blood panel analysis, which were conducted in the Drug Safety Evaluation Research Center (Shanghai

Institute of Materia Medica, Shanghai, China).

Hemolysis Analysis

Hemolysis assay was performed to evaluate the blood compatibility of nanocarrier (NbLipo).[19] Briefly, 3 mL blood taken from the mouse heart was mixed with 0.5 mL heparin solution (5 mg/mL). The erythrocytes were collected through centrifugation (1500 rpm, 15 min) and washed three times with 0.9% NaCl. Then, the supernatant liquid was removed, and 1mL erythrocytes was diluted to 50 mL with 0.9% NaCl to generate 2% erythrocyte solution. NbLipo and conventional liposomes (Lipo) dispersions were prepared in 0.9% NaCl at a concentration range of 125 ~ 1000 μg/mL. Then, 0.5 mL of NbLipo or Lipo solutions was added to 0.5 mL of erythrocyte solution, and the mixture was incubated at 37 °C for 3 h. Then, the mixture was centrifuged at 10000 rpm for 5 min. Hemolysis was measured at 570 nm via UV-vis of the supernatant. 0.9% NaCl and DI (deionized) water were included as negative and positive control, respectively.

Statistical Analysis.

Statistical analysis was conducted by using GraphPad Prism 7.0 software (La Jolla, CA). Differences between groups were examined using Student's *t*-test or ANOVA with Tukey's multiple comparison tests. Differences were considered significant if p-value was less than 0.05.

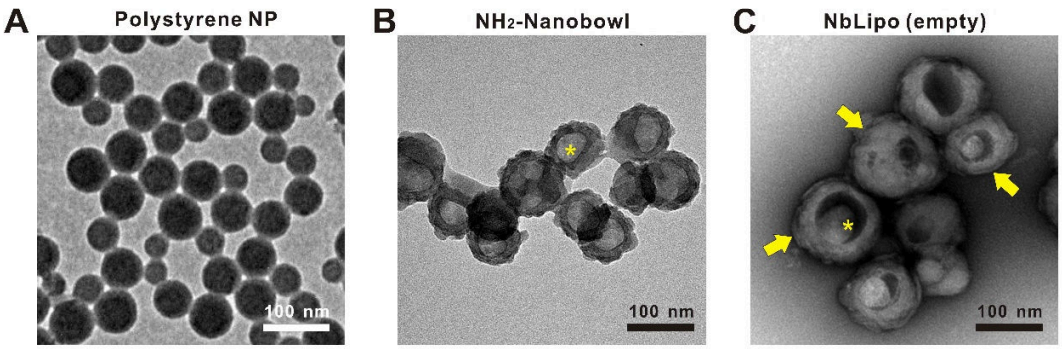

Figure S1. TEM of polystyrene NP (A), NH_2-Nanobowl (B), and NbLipo (empty) (C). In panel B and C, the nanobowl opening was indicated with yellow star, and the lipid bilayer was indicated with yellow arrows.

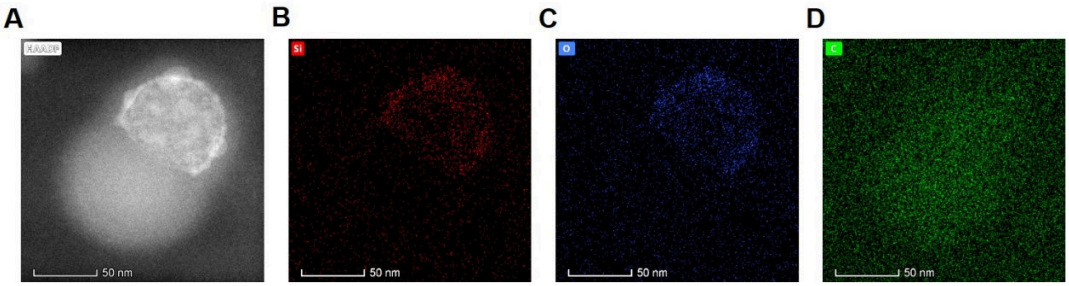

Figure S2. HAADF image (**A**) displayed a brighter signal with a cap-like morphology on the silica-coated hemisphere. EDS mapping indicated silicon (**B**) and oxygen (**C**) elements existed in the silica-coated hemisphere, while carbon (**D**) distribution in both hemispheres.

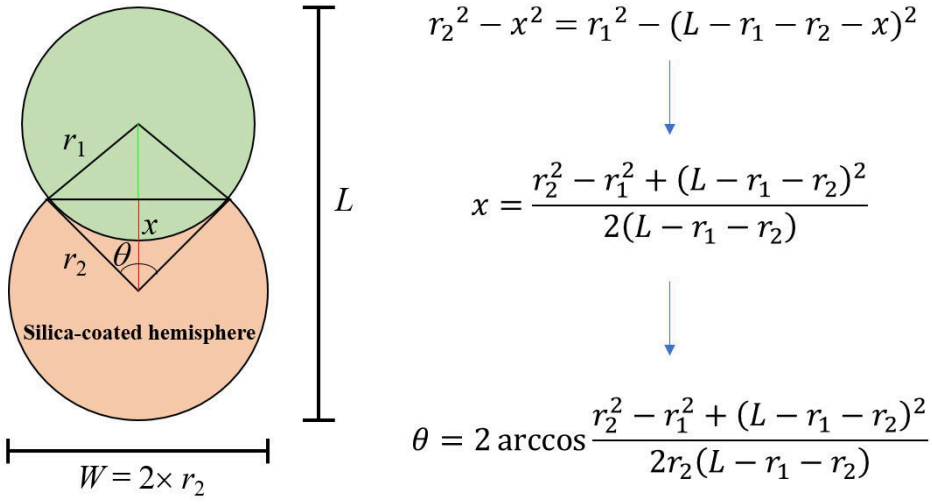

Figure S3. Estimation of the opening angel (θ) of nanobowls according to the dimension of silica-coated dumbbell using Pythagorean theorem.

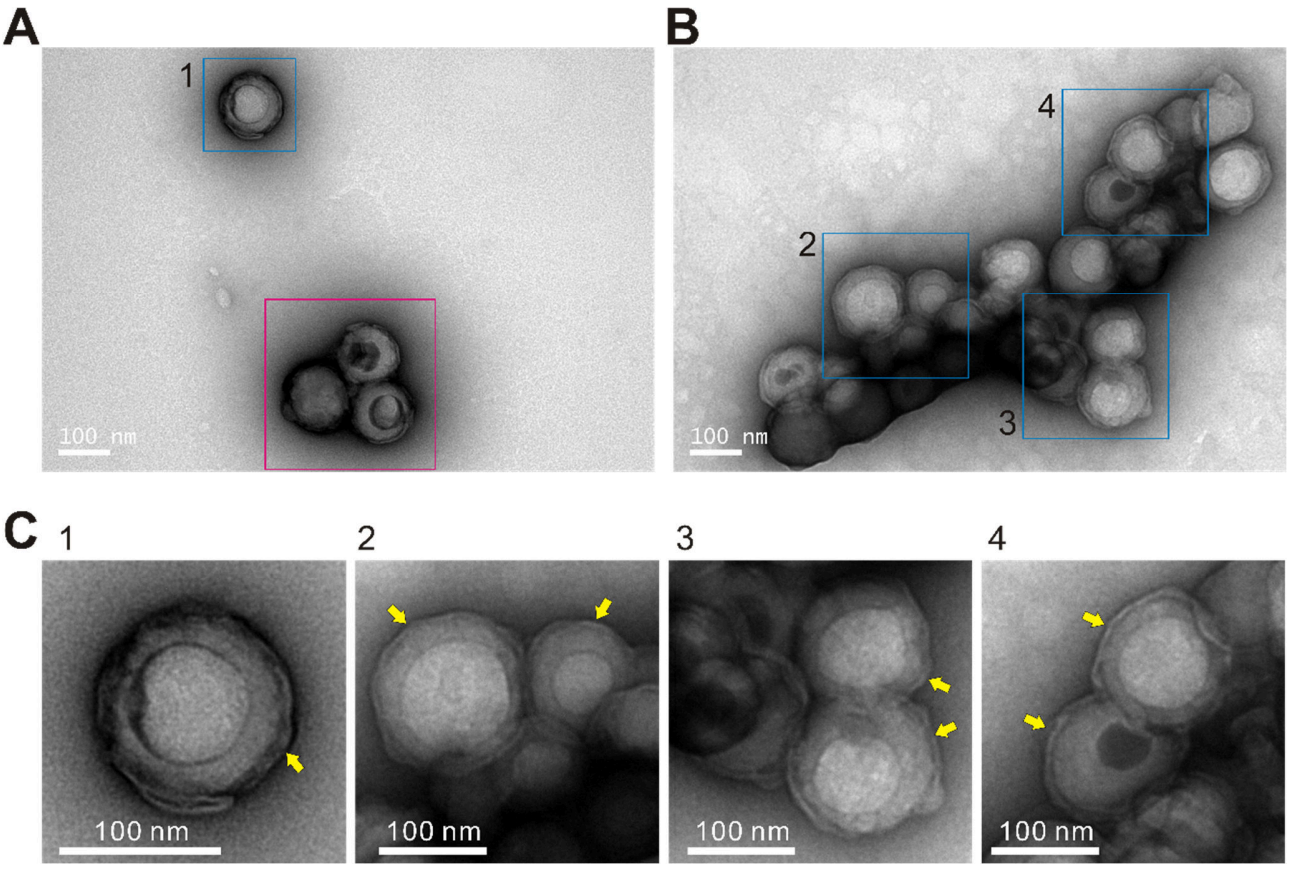

Figure S4. TEM images of other fields of DOX@NbLipo. The region in the blue box (#1, 2, 3, and 4) in **A** and **B** are magnified in **C**, respectively. The lipid bilayer was indicated with yellow arrow. The

region in the red box in A was also placed in the main text as Fig. 1E.

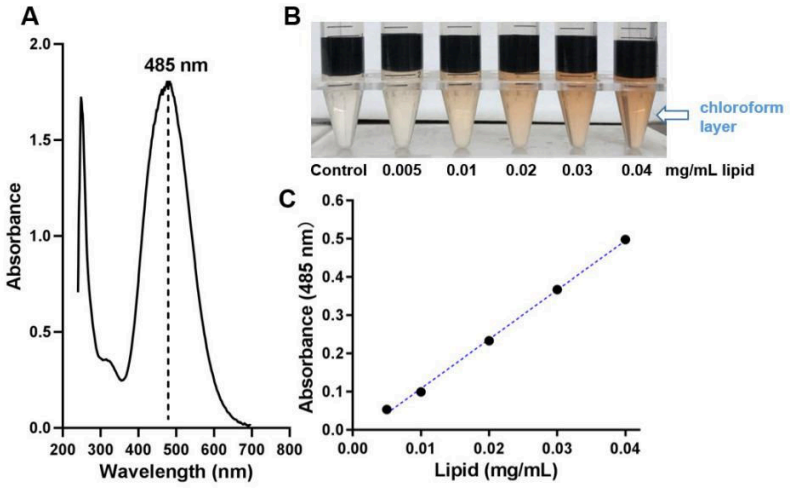

Figure S5. Lipid quantification. (**A**) Complex of ammonium ferrothiocyanate and phospholipids has a specific peak absorbance at 485 nm. (**B**) Complex standards in chloroform layer with different lipid concentrations. (**C**) Linear correlation between the absorbance value and the lipid content.

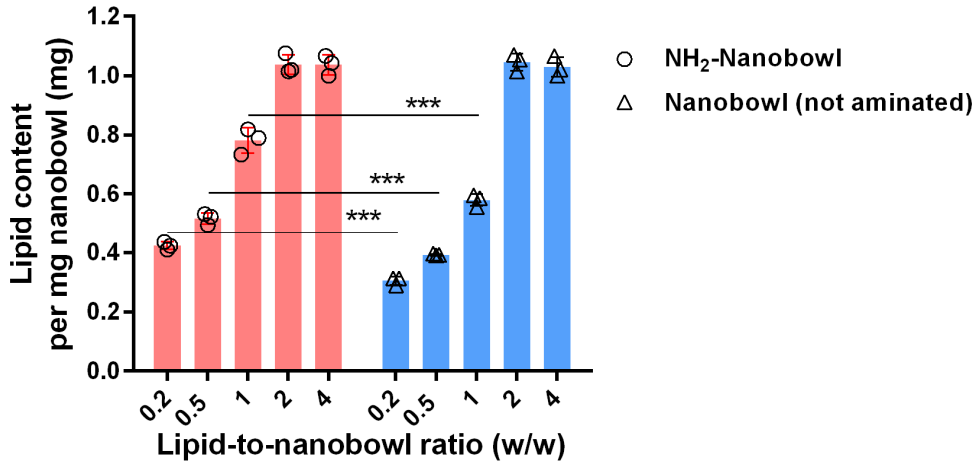

Figure S6. Detection of lipid content per mg nanobowl with the increase of lipid-to-nanobowl ratios (w/w). NH_2-Nanobowl and Nanobowl (not aminated) were used for NbLipo preparation, respectively. When lipid-to-nanobowl ratio went on above 2, the lipid content reached a platform value of ~ 1mg/mg

nanobowl. This also implied that all the nanobowls were wrapped with phospholipid.

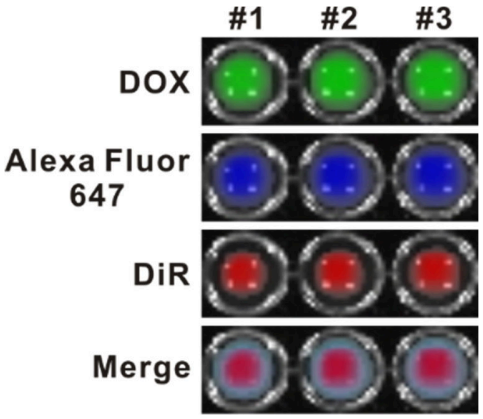

Figure S7. A dual-fluorophore-labeled DOX@NbLipo was prepared, in which NH_2-nanobowl was labeled with Alexa Fluor 647 NHS ester and lipid bilayer was labeled with DiR. DOX (Ex 490 nm, Em 590; green), Alexa Fluor 647 (Ex 650, Em 680; blue), and DiR (Ex 720 nm, Em 750 nm; red) contributed three fluorescent signals as observed in the IVIS spectrum CT instrument. The #2 sample was displayed in the inset of Figure 1H.

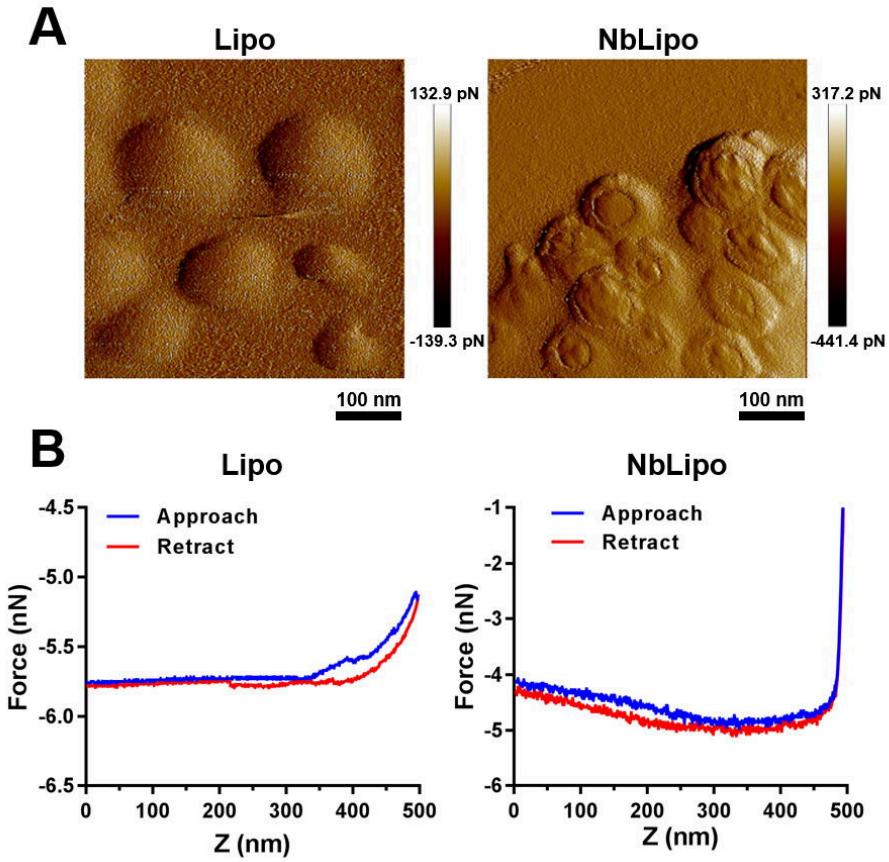

Figure S8. Elasticity of Lipo and NbLipo measured by AFM. (**A**) Representative AFM amplitude images of Lipo and NbLipo on poly-lysine coated megohmit. (**B**) Force-distance curves of the approaching and retracting processes obtained on Lipo and NbLipo.

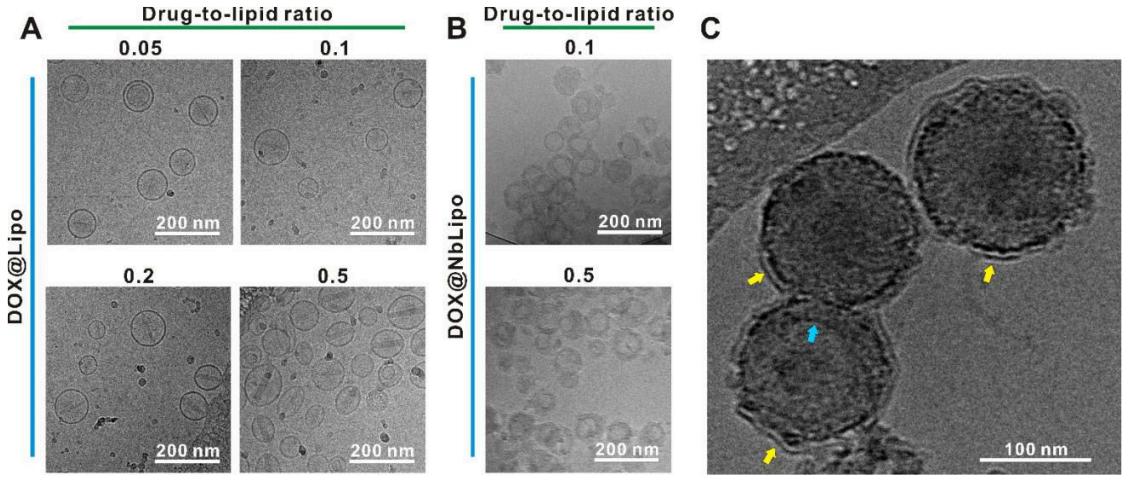

Figure S9. Cryo-EM photos of the DOX@Lipo (**A**) and DOX@NbLipo (**B**) at different drug-to-lipid ratios. (**C**) A magnified image of DOX@NbLipo at drug-to-lipid ratio (w/w) of 0.5 showed the lipid bilayer membrane on the surface. The lipid layer was indicated with yellow arrows, and the edge of a nanobowl opening was indicated with a blue arrow.

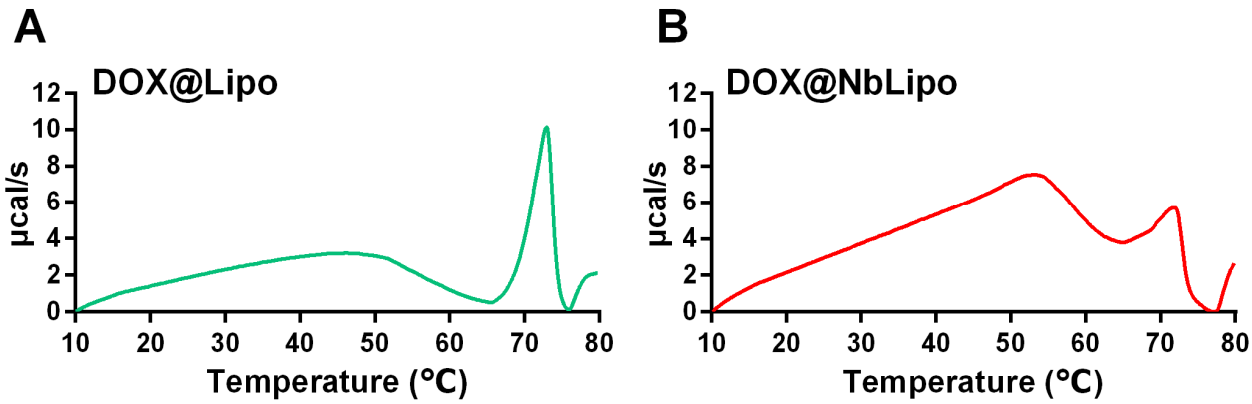

Figure S10. DSC assay of DOX@Lipo (1.76 mg/mL DOX) (**A**) and DOX@NbLipo (1.46 mg/mL DOX) (**B**). T_m at ~50 °C represented the membrane lipid phase transition, and T_m at ~72 °C reflected melting of the intraliposomal doxorubicin-sulfate nanocrystals.

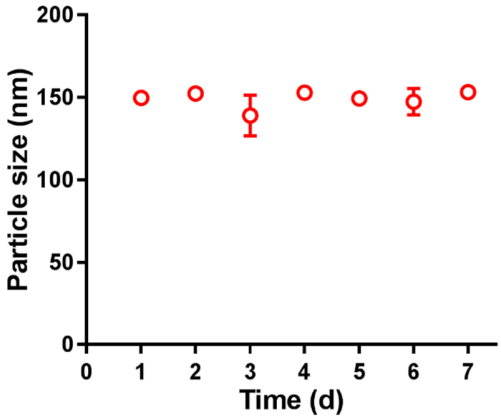

Figure S11. Colloid stability of DOX@NbLipo in pH 7.4 PBS at 4 ℃. Data represent mean ± s.d. (n= 3)

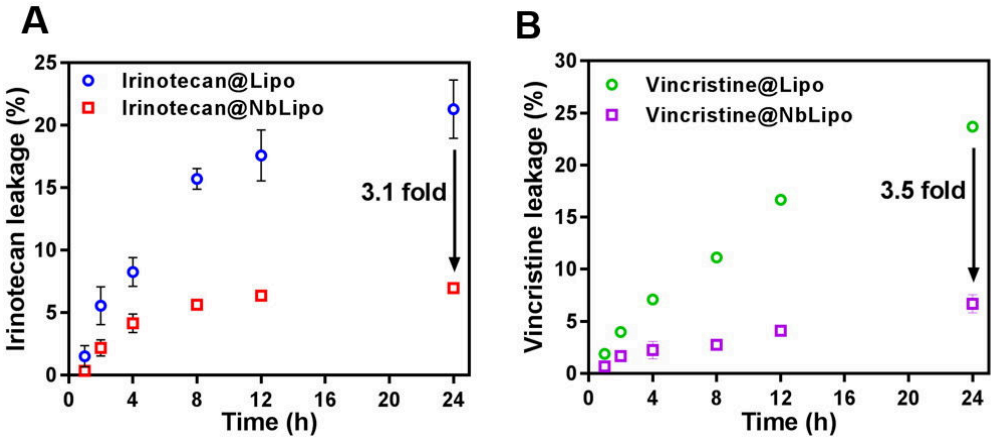

Figure S12. Drug leakage from irinotecan (**A**) or vincristine (**B**)-loaded Lipo and NbLipo. The drug-to-lipid ratio (w/w) was 0.2 for liposomal irinotecan and 0.4 for liposomal vincristine.

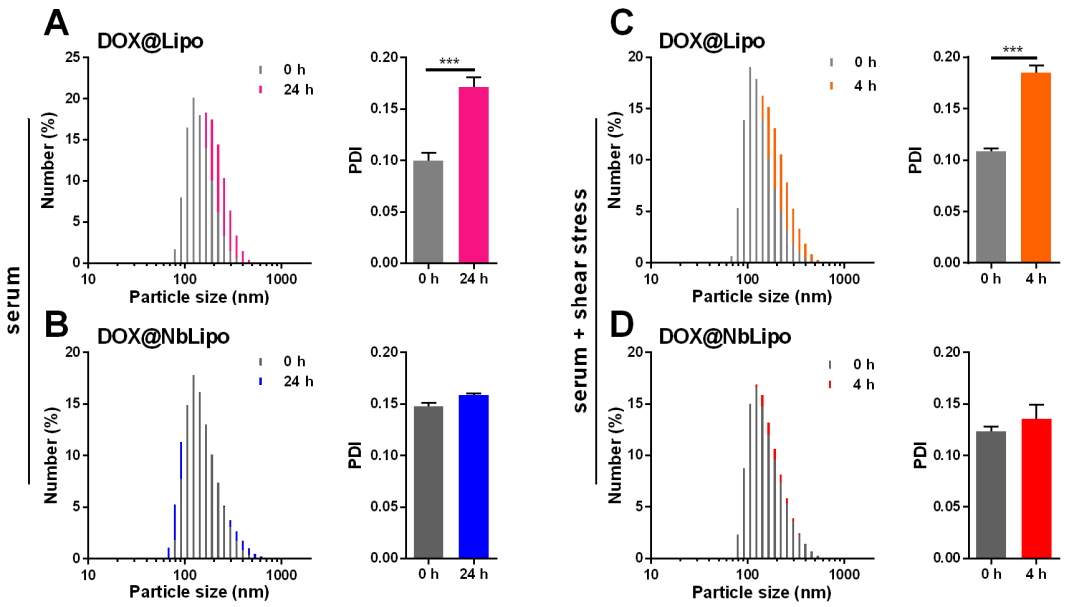

Figure S13. Size distribution and PDI (polydispersity index) of DOX@Lipo and DOX@NbLipo after incubation in serum (**A, B**) or serum plus shear stress (**C, D**). *** $p < 0.001$.

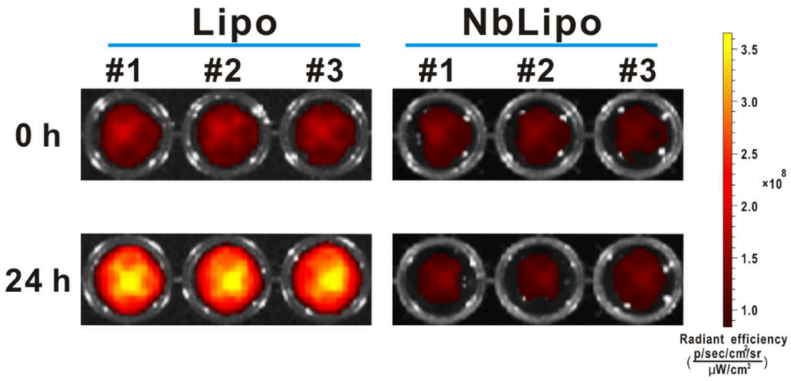

Figure S14. Enhanced FRET signal, using DiO-DiI donor-acceptor fluorophore pair, was observed in Lipo, but not NbLipo, after 24 h incubation in FBS. The samples at 0 and 24 h were placed in the 96-well plate and images were acquired at Ex 430 nm and Em 560 nm under the IVIS spectrum CT instrument.

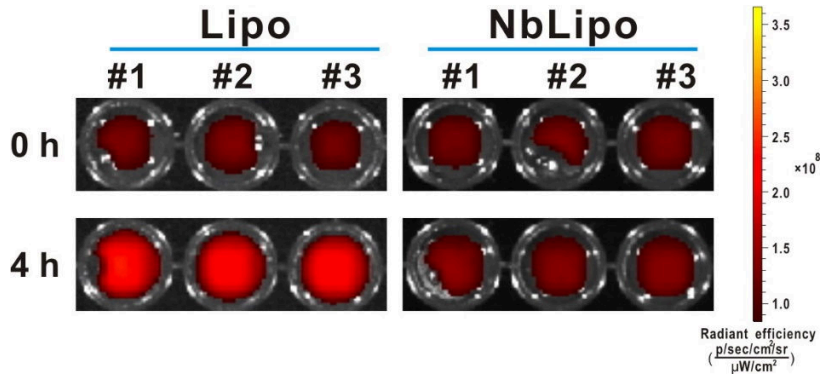

Figure S15. More enhanced FRET signal, using DiO-DiI donor-acceptor fluorophore pair, was observed in Lipo compared to that in NbLipo after 4 h treatment in FBS plus shear stress. The samples at 0 and 4 h were placed in the 96-well plate and images were acquired at Ex 430 nm and Em 560 nm under the IVIS spectrum CT instrument.

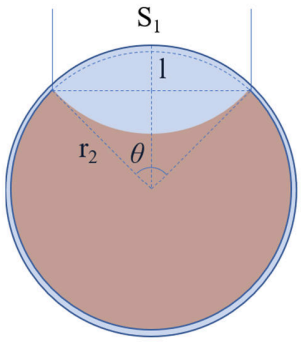

$$When\ \theta = 90°,\ l = r_2 - \frac{\sqrt{2}}{2}r_2$$

$$S_1 = 2\pi r_2 l = 2\pi r_2 \left(r_2 - \frac{\sqrt{2}}{2}r_2\right)$$

$$S_{all} = 4\pi r_2^2$$

$$\frac{S_1}{S_{all}} = \frac{2\pi r_2 \left(r_2 - \frac{\sqrt{2}}{2}r_2\right)}{4\pi r_2^2} = \frac{2-\sqrt{2}}{4} \approx 14.64\ \%$$

$$When\ \theta = 110°,\ l = r_2 - \cos 55° r_2$$

$$S_1 = 2\pi r_2 l = 2\pi r_2 \left(r_2 - \cos 55° r_2\right)$$

$$S_{all} = 4\pi r_2^2$$

$$\frac{S_1}{S_{all}} = \frac{2\pi r_2 \left(r_2 - \cos 55° r_2\right)}{4\pi r_2^2} = \frac{1-\cos 55°}{2} \approx 21.32\%$$

Figure S16. Estimation of the nanobowl opening area (S_1), which is also the liposome's inner surface area for cargo leakage. l, chord height; θ, nanobowl opening angle; r_2, radius of the sphere; S_{all}, surface area of the sphere.

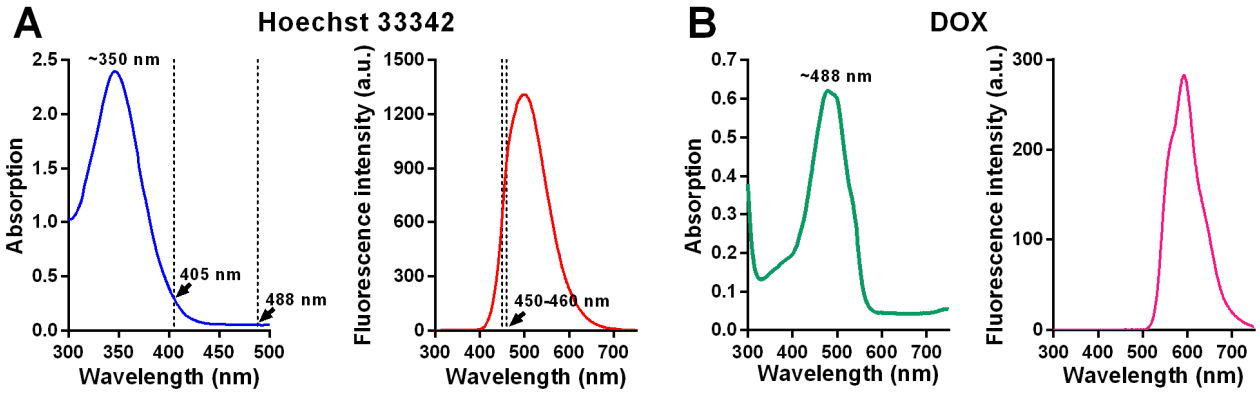

Figure S17. Absorption and emission spectra of Hoechst 33342 (A) and DOX (B). For cellular uptake assay, Hoechst 33342 was excited at 405 nm and observed at 450~460 nm, and DOX was at 488 nm and detected at 590 nm.

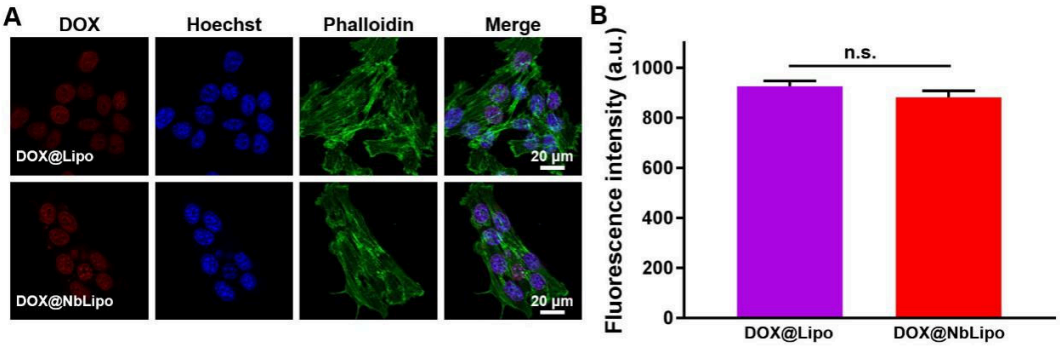

Figure S18. Cell uptake after 2 h incubation with the liposomes at 37 °C. (A) CLSM image of cellular uptake of the liposomes in 4T1 cells. (B) Quantified cell-associated DOX fluorescence intensity (Ex: 488 nm, Em: 585 nm) using flow cytometry.

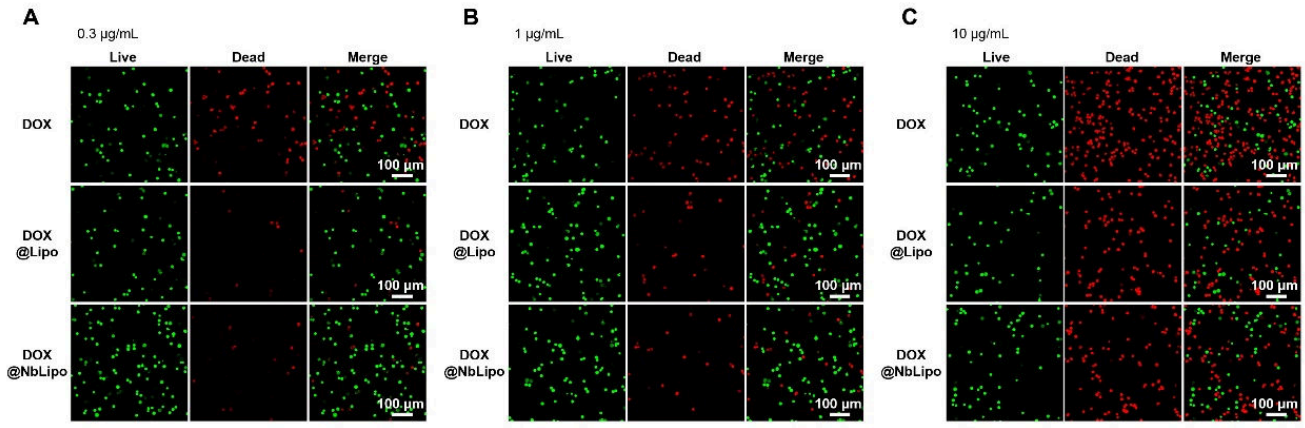

Figure S19. 4T1 cells treated with the various DOX formulations at DOX concentration of 0.3 (**A**), 1 (**B**), and 10 (**C**) μg/ml were stained with calcein-AM and 7-AAD for simultaneous fluorescence staining of viable and dead cells. The representative photographs of the cells were shown.

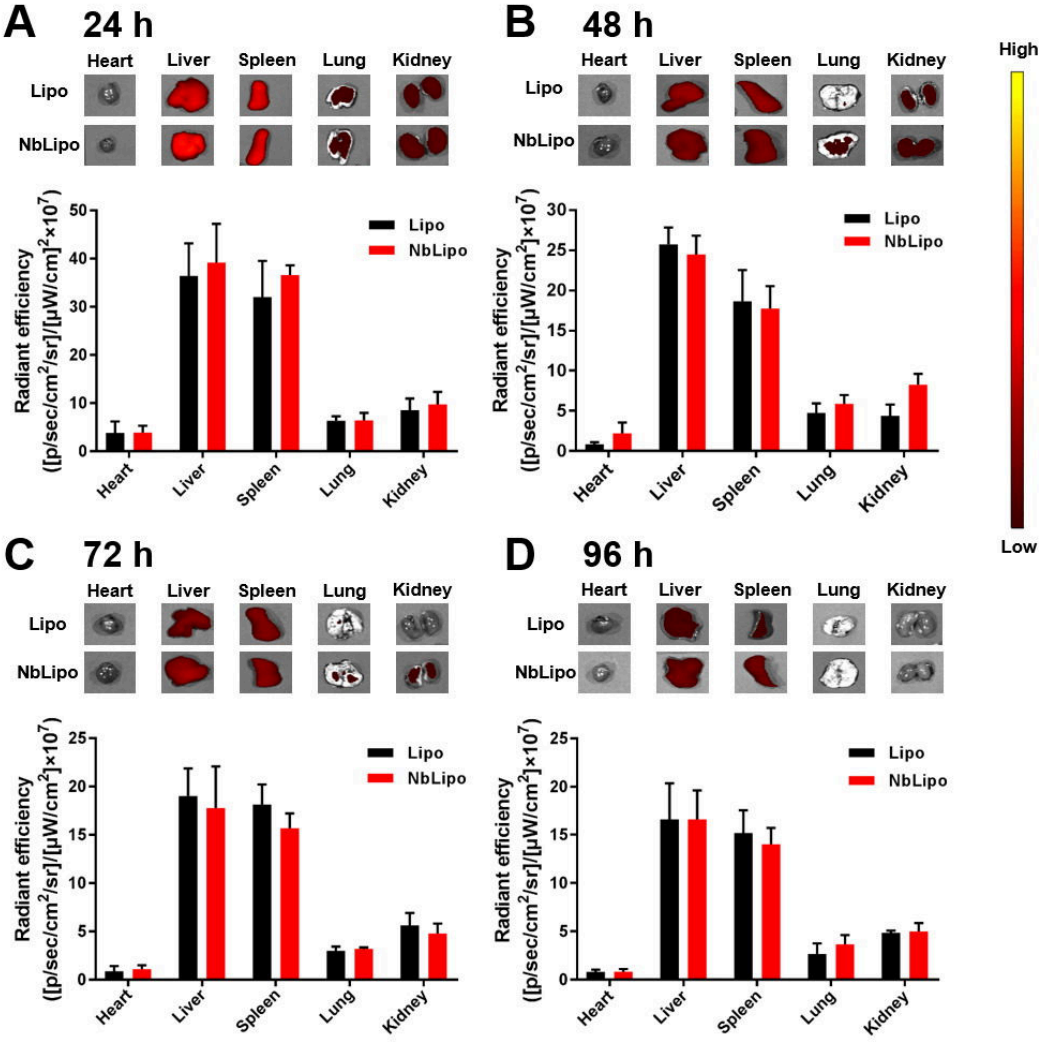

Figure S20. Statistical assay of the fluorescence intensity of DiD-labeled NbLipo or Lipo in major organs (heart, liver, spleen, lung, and kidney) at 24 h (**A**), 48 h (**B**), 72 h (**C**), and 96 h (**D**) after i.v. injection. Data are presented as mean ± s.d. (n = 3).

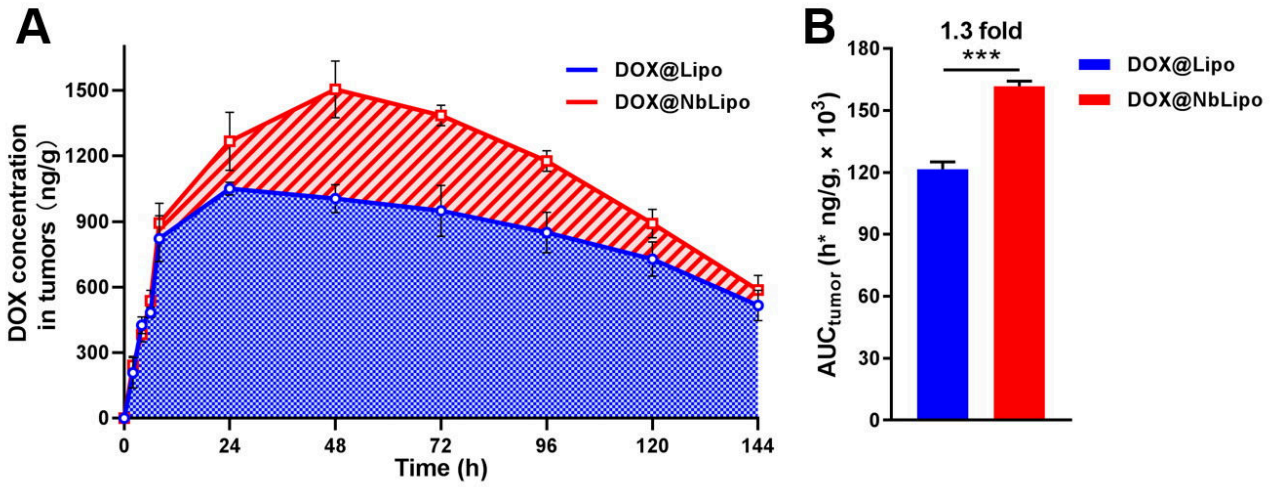

Figure S21. DOX pharmacokinetics in 4T1 tumors. (A) Time course of DOX concentration in 4T1 tumors. (B) DOX AUC in tumors calculated using WinNonlin software according to non-compartmental model. Values are expressed as mean ± SD, n= 5.

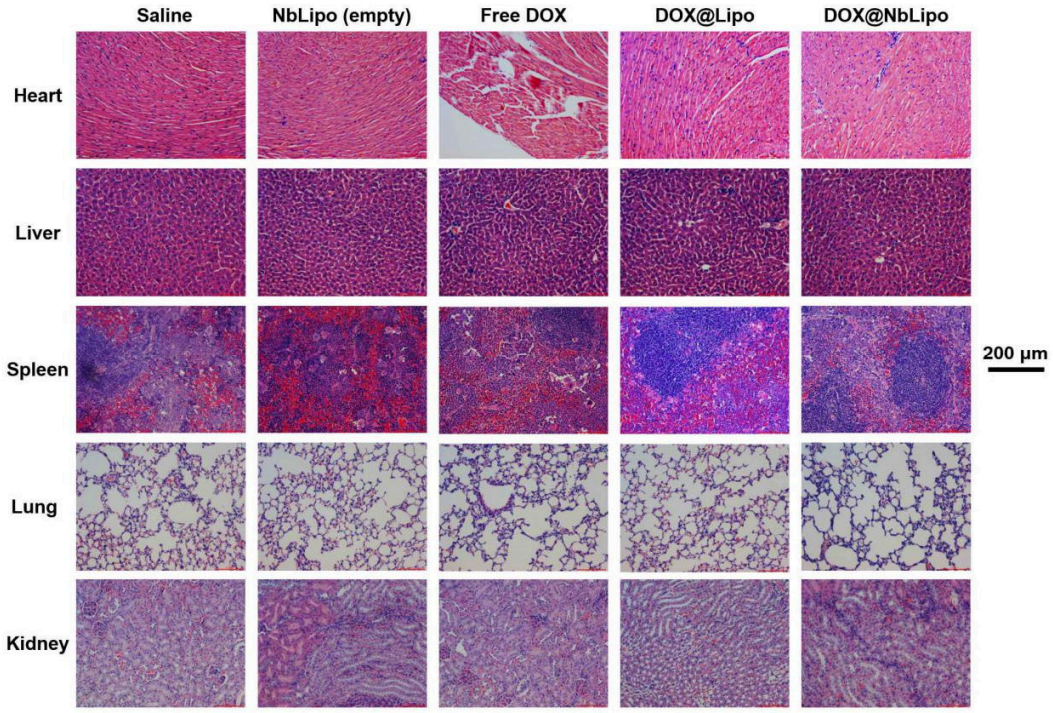

Figure S22. On day 7 (24 h after final injection of the liposomes), 3 mice from each group were sacrificed, and the major organs (heart, liver, spleen, lung, and kidney) of the mice were removed and processed for paraffin sections and histopathological examination (H&E staining).

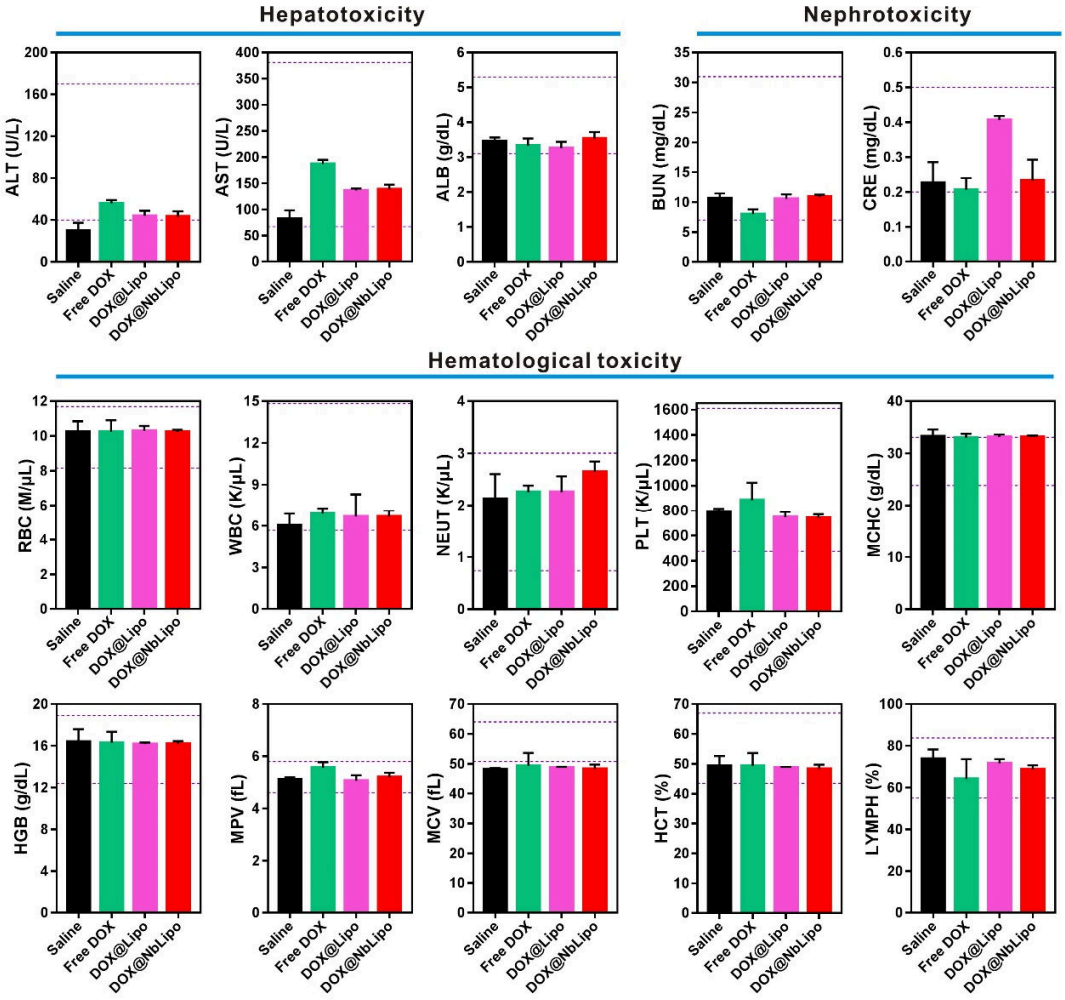

Figure S23. Toxicity profile of DOX@NbLipo in healthy female Balb/c mice. The liposomes were i.v. injected to the mice at 4 mg/kg on day 0, 3, and 6, respectively. 48 h after the third injection, the blood was collected from the mouse orbital for serum biochemistry and complete blood panel analysis. Reference ranges of hematology data (indicated with dotted line) were obtained from Charles River Laboratories (http://www.criver.com/). Three mice were used in each group for this experiment.

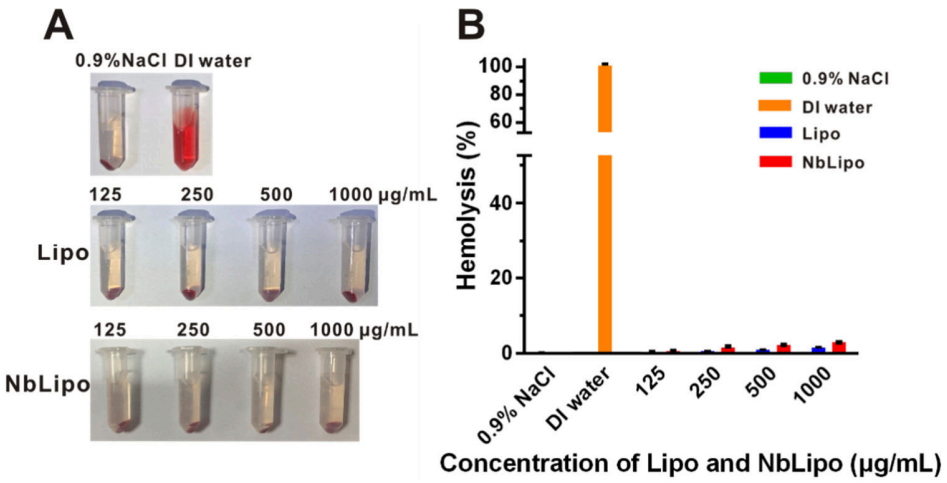

Figure S24. Hemolysis assay. (**A**) Photographs of the hemolysis tests. Blood cells were treated with 0.9% NaCl (negative control), DI (deionized) water (positive control), and different concentrations of Lipo and NbLipo for 3 h at 37 °C. (**B**) Hemolytic percentage. n =3.

Table S1. Noncompartmental pharmacokinetic parameters of free DOX, DOX@Lipo and DOX@NbLipo.

	$T_{1/2}$ (h) [a]	C_{max} (μg/ml)[b]	AUC_{0-48} (h*μg/ml)[c]	MRT_{0-48} (h)[d]	Cl (ml/h/g)[e]	Vz (ml/g)[f]
Free DOX	1.3	0.2	0.3	1.3	12.7	23.7
DOX@Lipo	14.6	1.3	15.8	14.1	0.3	5.4
DOX@NbLipo	19.4	1.3	25.4	15.7	0.2	4.4

[a] $T_{1/2}$, half-life in plasma. [b] C_{max}, the maximum plasma concentration. [c] AUC, are under the curve. [d] MRT, Mean residence time. [e] Cl, clearance. [f] Vz, volume of distribution.

Table S2. Survival analysis of the mice with various treatment.

	Median survival (day)	*ILS* (day) [a]	% *ILS* [b]
Saline	24	-	-
NbLipo (empty)	24	0	0
Free DOX	27	3	12.5
DOX@Lipo	30	6	25
DOX@NbLipo	50	26	108.3

[a] *ILS*: Increase in Life Span (*T* - *C*), where *T* and *C* are the mean survival time of treated mice and control mice from the saline group.

[b] $\%ILS = (T/C\text{-}1)\times 100\%$

References

1. Guignard, F.; Lattuada, M. Template-assisted synthesis of Janus silica nanobowls. *Langmuir* **2015,** *31* (16), 4635-4643.

2. De La Rosa, L. V.; Sudol, E. D.; El-Aasser, M. S.; Klein, A. Emulsion polymerization of styrene using reaction calorimeter. I. Above and below critical micelle concentration. *J. Polym. Sci. Pol. Chem.* **1999,** *37* (22), 4054-4065.

3. De La Rosa, L. V.; Sudol, E. D.; El-Aasser, M. S.; Klein, A. Emulsion polymerization of styrene using reaction calorimeter. II. Importance of maximum in rate of polymerization. *J. Polym. Sci. Pol. Chem.* **1999,** *37* (22), 4066-4072.

4. De La Rosa, L. V.; Sudol, E. D.; El-Aasser, M. S.; Klein, A. Emulsion polymerization of styrene

using reaction calorimeter. III. Effect of initial monomer/water ratio. *J. Polym. Sci. Pol. Chem.* **1999,** *37* (22), 4073-4089.

5. Stewart, J. C. Colorimetric determination of phospholipids with ammonium ferrothiocyanate. *Anal. Biochem.* **1980,** *104* (1), 10-14.

6. Shibata, H.; Yomota, C.; Okuda, H. Simultaneous determination of polyethylene glycol-conjugated liposome components by using reversed-phase high-performance liquid chromatography with UV and evaporative light scattering detection. *AAPS PharmSciTech* **2013,** *14* (2), 811-817.

7. Liu, X.; Situ, A.; Kang, Y.; Villabroza, K. R.; Liao, Y.; Chang, C. H.; Donahue, T.; Nel, A. E.; Meng, H. Irinotecan Delivery by Lipid-Coated Mesoporous Silica Nanoparticles Shows Improved Efficacy and Safety over Liposomes for Pancreatic Cancer. *ACS Nano* **2016,** *10* (2), 2702-2715.

8. Bulbake, U.; Doppalapudi, S.; Kommineni, N.; Khan, W. Liposomal Formulations in Clinical Use: An Updated Review. *Pharmaceutics* **2017,** *9* (2), 12.

9. Liang, Q.; Bie, N.; Yong, T.; Tang, K.; Shi, X.; Wei, Z.; Jia, H.; Zhang, X.; Zhao, H.; Huang, W.; Gan, L.; Huang, B.; Yang, X. The softness of tumour-cell-derived microparticles regulates their drug-delivery efficiency. *Nat. Biomed. Eng.* **2019,** *3* (9), 729-740.

10. Dai, Z.; Yu, M.; Yi, X.; Wu, Z.; Tian, F.; Miao, Y.; Song, W.; He, S.; Ahmad, E.; Guo, S.; Zhu, C.; Zhang, X.; Li, Y.; Shi, X.; Wang, R.; Gan, Y. Chain-Length- and Saturation-Tuned Mechanics of Fluid Nanovesicles Direct Tumor Delivery. *ACS Nano* **2019,** *13* (7), 7676-7689.

11. Wei, X.; Cohen, R.; Barenholz, Y. Insights into composition/structure/function relationships of Doxil(R) gained from "high-sensitivity" differential scanning calorimetry. *Eur. J. Pharm. Biopharm.* **2016,** *104*, 260-270.

12. Miranda, D.; Carter, K.; Luo, D.; Shao, S.; Geng, J.; Li, C.; Chitgupi, U.; Turowski, S. G.; Li, N.;

Atilla-Gokcumen, G. E.; Spernyak, J. A.; Lovell, J. F. Multifunctional Liposomes for Image-Guided Intratumoral Chemo-Phototherapy. *Adv. Healthc. Mater.* **2017,** *6* (16), 1700253.

13. Sakariassen, K. S.; Orning, L.; Turitto, V. T. The impact of blood shear rate on arterial thrombus formation. *Future Sci. OA* **2015,** *1* (4), Fso30.

14. King, M. A. Detection of dead cells and measurement of cell killing by flow cytometry. *J. Immunol. Methods* **2000,** *243* (1-2), 155-166.

15. Luo, D.; Goel, S.; Liu, H. J.; Carter, K. A.; Jiang, D.; Geng, J.; Kutyreff, C. J.; Engle, J. W.; Huang, W. C.; Shao, S.; Fang, C.; Cai, W.; Lovell, J. F. Intrabilayer ^{64}Cu Labeling of Photoactivatable, Doxorubicin-Loaded Stealth Liposomes. *ACS Nano* **2017,** *11* (12), 12482-12491.

16. Upadhyay, K. K.; Mishra, A. K.; Chuttani, K.; Kaul, A.; Schatz, C.; Le Meins, J. F.; Misra, A.; Lecommandoux, S. The in vivo behavior and antitumor activity of doxorubicin-loaded poly(gamma-benzyl l-glutamate)-block-hyaluronan polymersomes in Ehrlich ascites tumor-bearing BalB/c mice. *Nanomed- Nanotechnol. Biol. Med.* **2012,** *8* (1), 71-80.

17. Li, H. J.; Du, J. Z.; Du, X. J.; Xu, C. F.; Sun, C. Y.; Wang, H. X.; Cao, Z. T.; Yang, X. Z.; Zhu, Y. H.; Nie, S.; Wang, J. Stimuli-responsive clustered nanoparticles for improved tumor penetration and therapeutic efficacy. *Proc. Natl. Acad. Sci. U.S.A.* **2016,** *113* (15), 4164-4169.

18. Dong, X.; Liu, H. J.; Feng, H. Y.; Yang, S. C.; Liu, X. L.; Lai, X.; Lu, Q.; Lovell, J. F.; Chen, H. Z.; Fang, C. Enhanced Drug Delivery by Nanoscale Integration of a Nitric Oxide Donor To Induce Tumor Collagen Depletion. *Nano Lett.* **2019,** *19* (2), 997-1008.

19. Jin, Y.; Liang, X.; An, Y.; Dai, Z. Microwave-Triggered Smart Drug Release from Liposomes Co-encapsulating Doxorubicin and Salt for Local Combined Hyperthermia and Chemotherapy of Cancer. *Bioconjug. Chem.* **2016,** *27* (12), 2931-2942.